



Cite this: *Org. Biomol. Chem.*, 2017, **15**, 459

Improving cell penetration of helical peptides stabilized by N-terminal crosslinked aspartic acids†

Hui Zhao,^a Yanhong Jiang,^a Yuan Tian,^b Dan Yang,^a Xuan Qin^a and Zigang Li^{*a}

Received 16th November 2016,
Accepted 30th November 2016
DOI: 10.1039/c6ob02501c

www.rsc.org/obc

Cell penetration and nucleus translocation efficiency are important for the cellular activities of peptide therapeutics. For helical peptides stabilized by N-terminal crosslinked aspartic acid, correlations between their penetration efficiency/nucleus translocation and physicochemical properties were studied. An increase in hydrophobicity and isoelectric point will promote cellular uptake and nucleus translocation of stabilized helices.

Introduction

A number of vital biological processes are mediated by protein–protein interactions (PPIs),^{1,2} which generally feature large and complex surfaces. Stabilized amphiphilic helical peptides^{3–7} were broadly utilized to modulate PPIs, thanks to their enhanced proteolytic resistance and cell penetration.⁸ However, when addressing intranuclear targets,⁹ one major problem is the nucleus translocation efficiency of stabilized peptides.¹⁰ Therefore, investigating the correlation between different physicochemical properties of peptides and their cell penetration or nucleus translocation will underlie generation of helices with higher nucleus accumulation. Parang *et al.* reported that homochiral cyclic peptides composed of Trp and Arg could be used as efficient nucleus-targeting molecular transporters.¹¹ Cardoso *et al.* elucidated the molecular requirements for proteins to target the nucleolus.¹² However, criteria of evaluating the nucleus translocation efficiency of stabilized amphiphilic helices are still not well studied.

Recently, we developed a helix nucleating template based on cross linked aspartic acids (terminal aspartic acid, TD) (Fig. 1).¹³ Unlike most nucleating strategies, the on-tether N-terminal amino group is preserved to enable further modifications. In addition, the TD strategy increases permeability mainly *via* conformation constraining rather than lipophilicity tuning.¹⁴ Thus, the TD strategy provides a good platform to

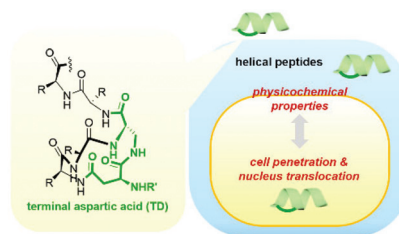


Fig. 1 Correlations between physicochemical properties and cell penetration or nucleus translocation for terminal aspartic acid (TD) stabilized helices.

study how mutations in short helices affect their cell penetration and translocation into the nucleus.

Herein, a panel of amphiphilic helical peptides were synthesized and investigated. We first quantified the permeability of these peptides and determined their membrane-penetration mechanism using fluorescence activated cell sorting (FACS). Then based on the analysis of confocal imaging data, we obtained relative nucleus accumulation of the peptides. Finally, the correlation between cell penetration/nucleus translocation and theoretical physicochemical coefficients were evaluated. As a brief summary of this study, residues like Trp, Phe and Arg are more favoured than His, Met, Val, and Tyr for cell penetration or nucleus translocation. The hydrophobicity and isoelectric point of helical peptides are the driving forces for their cell penetration and nucleus accumulation. This study helps to understand and predict cell penetration or nucleus translocation of TD stabilized helical peptides, and may also help in designing more efficient cell penetrating or nucleus targeting helical peptides.^{15,16}

^aSchool of Chemical Biology and Biotechnology, Peking University Shenzhen Graduate School, Shenzhen, 518055, China. E-mail: lizg@pkusz.edu.cn

^bSchool of Life Science and Engineering, Southwest Jiaotong University, Chengdu, 611756, China

†Electronic supplementary information (ESI) available. See DOI: 10.1039/c6ob02501c

Results and discussion

A typical amphiphilic peptide **0** was chosen as our model template as most helical PPI modulators are amphiphilic (Fig. 2). Cationic amino acids are of great importance for nuclear uptake.¹² In addition to peptides' formal charges, Walensky *et al.* recently reported that for stapled peptides, staple placement, optimal hydrophobicity and helical contents count for peptides' cellular uptake synergistically.¹⁷ Collectively, we focused on the mutations of basic and hydrophobic amino acids in the model peptide (Arg and Leu) to investigate the impact of physicochemical properties on cell penetration or nucleus translocation. We synthesized peptide (Table S1 and Fig. S1†) analogues as shown in Fig. 2. These peptides exhibit a helical conformation according to circular dichroism (CD) spectroscopy (Fig. 2). A Leu containing peptide (**0**) favours helical conformations compared to peptides composed of other hydrophobic amino acids.

Then MCF-7 cells were treated with our peptides and the peptides' cellular uptake was quantified by FACS (Fig. 3A). For peptides with basic amino acid mutations, the penetration ranking is Arg (**0**) > Lys (**2-K**) ≈ His (**2-H**), while for those with hydrophobic amino acid mutations, the penetration ranking is Trp (**3-W**) > Phe (**3-F**) > Leu (**0**) > Tyr (**3-Y**) > Val (**3-V**) ≈ Met (**3-M**). The ranking is consistent with the previous reports of Trp and Arg as penetration-promoting residues.^{18,19} The natural linear peptide **0_{lin}** showed low cell penetration compared to the cyclic counterpart (Fig. 3A). Since cell membrane compositions differ between cell lines,²⁰ cellular uptake by HEK293T was then examined for comparison (Fig. 3B). The results on two cell lines were basically consistent (Pearson correlation coefficient = 0.975, $p < 0.01$), suggesting that the cell penetration of TD stabilized helices is closely related to residues. Notably, for TD peptides, no clear correlation can be observed between the helicity of peptides and their cellular uptake, suggesting that factors other than the rigidity of peptides contribute more to cell penetration.

Then we investigated the mechanism responsible for cellular uptake using a series of inhibitors as shown in Fig. 3C and Table S2.† Amiloride (1, inhibitor of macropinocytosis) and Nystatin (4, inhibitor of caveolae-mediated endocytosis) induce

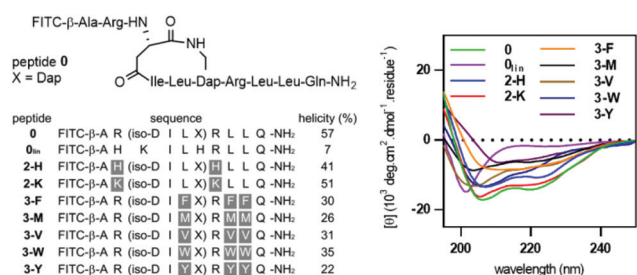


Fig. 2 Peptide sequences, circular dichroism spectra and calculated helicity (%) of peptides in 35% CH₃CN/PBS (10 mM, pH 7.4, 298 K, concentration normalised). Dap = 2,3-diaminopropionic acid, FITC = fluorescein isothiocyanate, PBS = phosphate buffer saline.

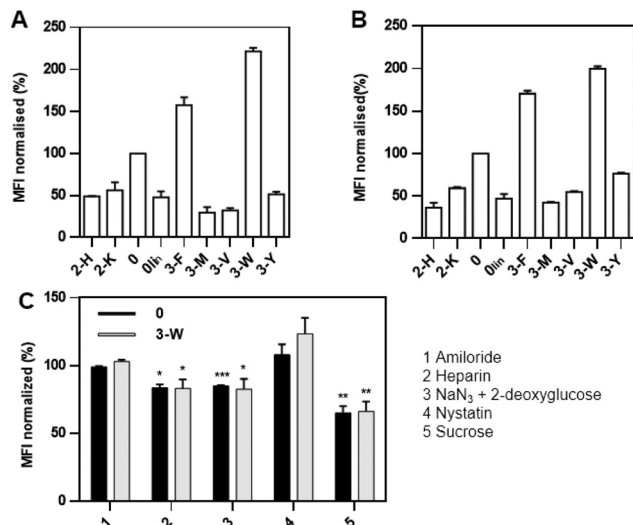


Fig. 3 Cellular uptake of peptides. Normalised mean fluorescence intensity (MFI) of (A) MCF-7 and (B) HEK293T cell lines treated with peptides (5 μM, 310 K, 1 h). All values were normalised to that of **0** (5 μM, 310 K, 1 h). (C) Effects of various inhibitors on the internalization of **0** and **3-W** (MCF-7, 5 μM, 310 K, 1 h). All values were normalised to that of **0** or **3-W** without inhibitors, respectively. Error bars represent the standard error of mean from more than two independent experiments. * $p < 0.05$, ** $p < 0.01$, and *** $p < 0.001$.

no decrease in cellular uptake, suggesting that the penetration of peptides is macropinocytosis and caveolae-mediated endocytosis independent. Reduction in penetration in cells treated with heparin (2) suggests the importance of the electrostatic interactions of peptides with the negatively charged phospholipid membrane. Also, reduced cellular uptake was observed upon a combination treatment with sodium azide and deoxyglucose (3) and sucrose (5) suggesting a mixed mechanism mainly involving clathrin-mediated endocytosis. The mechanism of cell penetration is different from the previous results of helical peptides,^{21,22} which enter cells mainly *via* a macropinocytotic mechanism.

Then we examined the cellular distribution of our peptides using confocal imaging (Fig. 4A). In general, peptides showed a stronger fluorescence intensity in the cytosol than the nucleus, suggesting that the nucleus membrane is indeed a barrier for nucleus accumulation of peptides. Then, nucleus/cell fluorescence ratios (N/C) in cross section were obtained using ImageJ. The N/C of peptides in the whole cell was then estimated and is summarized in Fig. 4B. Comparatively, a gap between N/Cs is not as significant as that between cell penetrations. Furthermore, we obtained the relative nucleus accumulation (Fig. 4C) by multiplying the above ratios with the mean cellular uptake obtained by FACS in Fig. 3A. Similar to the case of cell penetration, there is no observed correlation between the helicity of TD stabilized peptides and their nucleus targeting capacity. Furthermore, Trp (**3-W**), Phe (**3-F**), and Arg (**0**) are favourable for nucleus translocation, while Tyr (**3-Y**) is not.¹¹ Consistency between cellular uptake and nucleus accumulation (Pearson correlation coefficient = 0.992, $p < 0.01$)

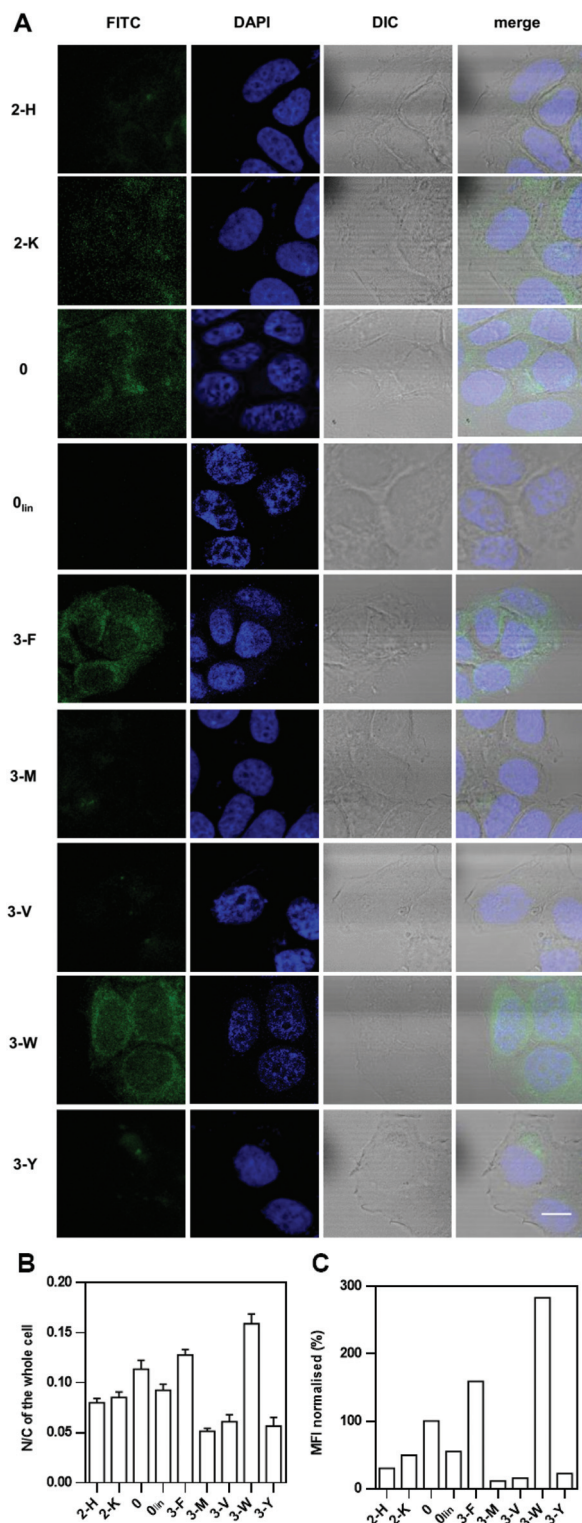


Fig. 4 Nucleus translocation of peptides. (A) Confocal microscopy images of the MCF-7 cells incubated with peptides (5 μ M) at 310 K for 4 h. Scale bar, 20 μ m. (B) Quantification of the ratio of the peptides fluorescence intensity per pixel into nucleus versus cell (N/C) using ImageJ. Results were presented as the ratio found per peptide for more than 10 cell population, from more than two independent experiments, and then calculated according to the function in the main text. Error bars represent the standard error of mean. (C) Estimated nucleus mean fluorescence intensity normalized to 0.

of these peptides suggests that nucleus translocation is largely dependent on the amount of peptides penetrated into the cells. Thus, the residues favourable for cell penetration are generally favourable for nucleus accumulation.

Then we analysed the correlation between biophysical properties¹⁷ and cell penetration and nucleus translocations. Properties including hydrophobicity (H) and isoelectric point (IP) were obtained for each peptide using calculating tools (Fig. 5A).²³ Finally, the cell penetration and the estimated nucleus accumulation obtained above were plotted against the estimated hydrophobicity and isoelectric point to investigate their correlations (Fig. 5B and C). For peptides with the same IP (peptide 0, 3-F, 3-M, 3-V, 3-W, 3-Y), strong positive correlations between the hydrophobicity and cell penetration ($R^2 = 0.88$) or nucleus accumulation ($R^2 = 0.91$) are observed (Fig. 5B). While for peptides whose basic residues were mutated, the isoelectric point shows a correlation with cell penetration ($R^2 = 0.69$) or nucleus translocation ($R^2 = 0.81$) (Fig. 5C). Furthermore, correlation analysis including all stabilized peptides derives no clear correlation between IP/ H alone and penetration/nucleus translocation, (Fig. S2†) indicating

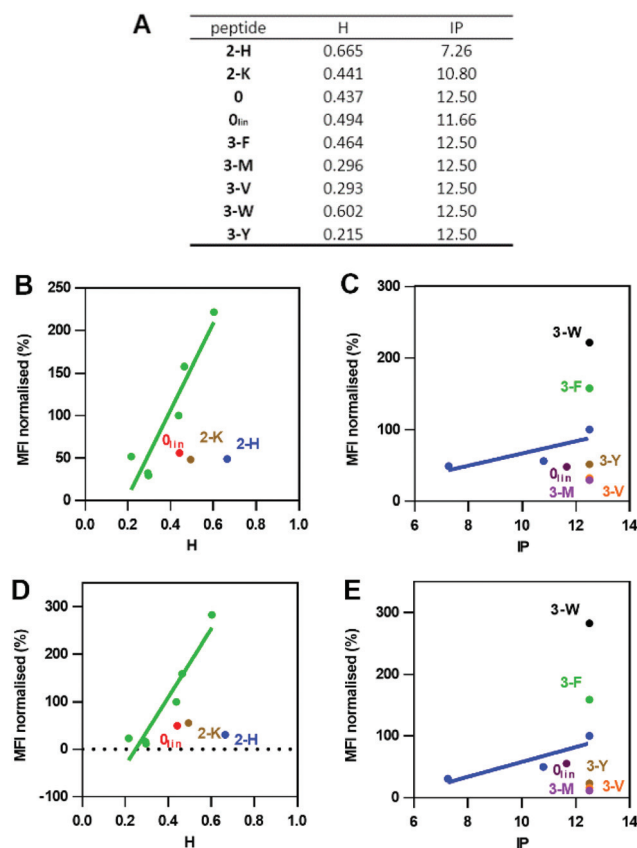


Fig. 5 Correlation between physicochemical properties and nucleus accumulation of peptides. (A) Theoretical physicochemical parameters of peptides. Correlation between (B) H (hydrophobicity, $R^2 = 0.88$), (C) IP (isoelectric point, $R^2 = 0.69$) and cell penetration of peptides. Correlation between (D) H (hydrophobicity, $R^2 = 0.91$), (E) IP (isoelectric point, $R^2 = 0.81$) and nucleus translocation of peptides.

that multiple regression might be suitable for correlation analysis. Accordingly, the relationship between physicochemical properties and cell penetration/nucleus accumulation was set up *via* binary regression [normalised cell penetration (NCP) (%) = $-564.5 + 512.4 \times H + 37.2 \times IP$, $R^2 = 0.89$; normalised nucleus translocation (NNT) (%) = $-824.9 + 721.0 \times H + 51.7 \times IP$, $R^2 = 0.92$]. The involvement of θ_{in} leads to the reduction of R^2 in two component regression analyses ($R^2 = 0.76$ for NCP, $R^2 = 0.84$ for NNT), suggesting that the correlation might be more suitable for TD stabilized peptides.

To sum up, higher hydrophobicity and IP are favourable factors for peptides' cell penetration and nucleus translocations.

To further test the hypothesis, we introduced two Trp/Arg-rich helical peptides, **4-R** and **4-W** (Fig. 6A and S3[†]), and obtained their cell penetration and nucleus translocation (Fig. 6B–D and S4[†]). For peptide **4-W**, higher hydrophobicity than **3-W** generates higher cell penetration and nucleus translocation, while for **4-R**, even higher nucleus accumulation, which features nucleolus accumulation,¹² is observed despite

its lower hydrophobicity. The extraordinary jump in nucleus penetration might be explained by the IP beyond 12.6, accompanied by a change of the nucleus targeting mechanism. Furthermore, the excellent cell penetration, nucleus translocation, and low toxicity (Fig. S5[†]) of **4-R** and **4-W** make them applicable for cellular delivery of cargos.

To sum up, increasing the hydrophobicity or isoelectric point of stabilized helices promotes their cell penetration and nucleus accumulation. Accordingly, mutations increasing their integral hydrophobicity and/or isoelectric point could be made to improve their cell penetration and nucleus translocation efficiency.

Experimental

Materials

All solvents and reagents used for solid phase peptide synthesis were purchased from commercial suppliers including GL Biochem (Shanghai) Ltd, Shanghai Hanhong Chemical Co., J&K Co. Ltd, Shenzhen Tenglong Logistics Co., or Energy Chemical Co., and were used without further purification unless otherwise stated.

Synthesis and characterization of peptides

Peptides were synthesized on Rink amide MBHA resin using manual Fmoc/*t*Bu solid-phase peptide synthesis (SPPS).¹³ Coupling reactions were performed using 2-(1*H*-6-chlorobenzotriazol-1-yl)-1,1,3,3-tetramethyluronium hexafluorophosphate or 1-hydroxybenzotriazole (HOBt)/*N,N'*-diisopropylcarbodiimide with N_2 bubbling. The allyl ester and allyl carbamate were removed using $Pd(PPh_3)_4$ (0.1 eq.) and *N,N*-dimethylbarbituric acid (4 eq.) twice in dichloromethane for 2 h. Cyclization was performed on the resin using benzotriazol-1-yl-oxytripyrrolidinophosphonium hexafluorophosphate/HOBt/*N*-methylmorpholine (2:2:2.4 eq.) in DMF. Fluorescein isothiocyanate (FITC) labelling was performed on the resin with a solution of FITC (isomer I, 4 eq.) and *N,N*-diisopropylethylamine (14 eq.) in *N,N*-dimethylformamide overnight. Finally resins were cleaved with 95% (v/v) trifluoroacetic acid (TFA)/triisopropylsilane/ H_2O (95:2.5:2.5) for 2 h. After air removal of most of the TFA, the products were triturated with hexane/diethyl ether (1:2), and then the precipitate was dissolved in CH_3CN/H_2O . Crude peptides were purified on a RP-HPLC (Waters 600, Agilent Zorbax SB-Aq: 4.6×250 mm, 220 nm & 254 nm) and confirmed by MS (Shimadzu LC-MS 2020).

Circular dichroism spectroscopy

CD spectra were obtained using a Chirascan plus circular dichroism spectrometer. Peptides were dissolved in 10 mM 35% CH_3CN/PBS (pH 7.4, 10 mM, pH 7.4, 298 K) at a concentration of 50 μM . Parameters used in the experiment are as follows: wavelengths from 250 to 190 nm were measured with a resolution of 0.5 nm, a response of 1 s, a bandwidth of 1 nm, and a scanning speed of 20 nm min^{-1} . Each spectrum

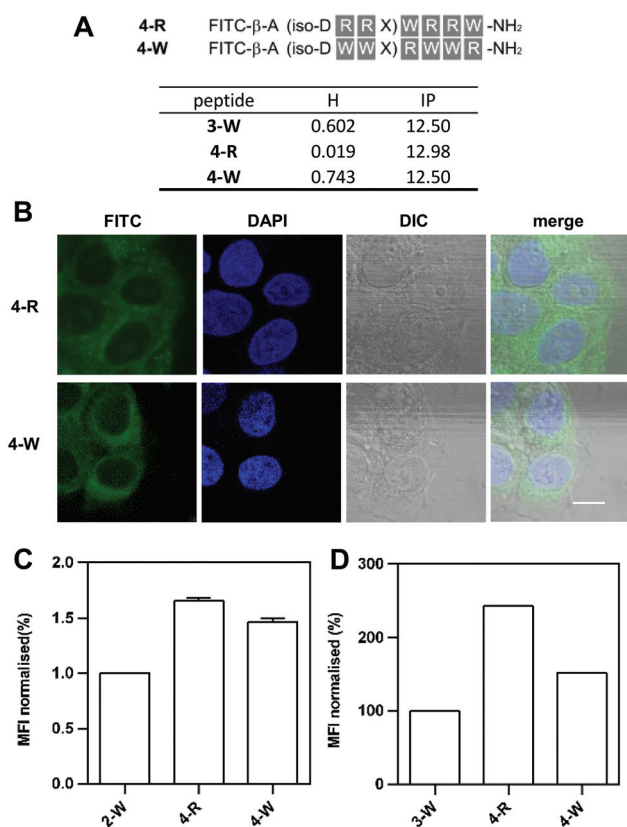


Fig. 6 Further evaluation of Arg and Trp rich peptides. (A) Theoretical physicochemical parameters of peptide **4-R** and **4-W**. (B) Confocal microscopy images of the MCF-7 cells incubated with peptides (5 μM) at 310 K for 4 h. Scale bar, 20 μm . (C) Normalised mean fluorescence intensity (MFI) of MCF-7 lines treated with peptides (5 μM , 310 K, 1 h). All values were normalised to that of **3-W** (5 μM , 310 K, 1 h). Error bars represent the standard error of mean from two independent experiments. (D) Estimated nucleus mean fluorescence intensity normalised to **3-W**.

represents the average of two scans and smoothed using ProData Viewer by Applied Photophysics with a smooth window of 10. CD data were presented as the mean residual ellipticity $[\theta]$ in $\text{deg cm}^2 \text{dmol}^{-1}$. Concentrations were determined as mentioned in general information. The percentage of helicity was theoretically calculated based on the equation:¹³ Helicity% = $[\theta]_{222}/[\theta]_{\text{max}} \times 100$, where $[\theta]_{\text{max}} = (-44\,000 + 250T)(1 - k/n)$ for $k = 4.0$ and $n =$ number of amino acid residues in the peptide, $T = 298 \text{ K}$.

Flow cytometry analysis

Adherent cells were seeded in 24-well plates and allowed to grow for 48 h in medium supplemented with 10% FBS. The cells were then treated with FITC-labelled peptides (5 μM without or with inhibitors, inhibitors are shown in Table S2†) in FBS-free medium for 1 h at 310 K. The peptide solution was removed and the cells were collected and washed with phosphate buffer saline (PBS) three times. Cellular mean fluorescence intensities were measured using a flow cytometer (BD FACSCalibur).

Confocal microscopy imaging

The adherent cells were seeded in 24-well plates on coverslips and allowed to grow for 48 h in medium supplemented with 10% FBS until experiment. The cells were then treated with the FITC-labelled peptide for 4 h at 310 K in the presence of 5% CO_2 followed by washing with PBS and fixed with 4% paraformaldehyde in PBS for 25 min at room temperature. Then the coverslips were mounted on slides upside down with mounting medium (VECTASHIELD) containing 4',6-diamidino-2-phenylindole (DAPI). The samples were imaged using a confocal microscope (Zeiss, LSM510 META). Acquired images were then analysed by using open source software ImageJ. The N/C in the cross section could be obtained using ImageJ.

To estimate the N/C of the whole cell, we simplified the nucleuses and cells into uniformly fluorescent spheres. We set the radius of the nucleus and the whole cell as r and R respectively. Also, we set the fluorescence (amount of peptide) per unit distance of the nucleus and the whole cell as Δf and ΔF . Thus the N/C in the cross section could be expressed as:

$$\frac{\pi r^2 \times \Delta f^2}{\pi R^2 \times \Delta F^2}$$

Accordingly, the N/C of the whole cell is:

$$\frac{\frac{4}{3}\pi r^3 \times \Delta f^3}{\frac{4}{3}\pi R^3 \times \Delta F^3} = \left(\sqrt{\frac{\pi r^2 \times \Delta f^2}{\pi R^2 \times \Delta F^2}} \right)^3$$

Theoretical physicochemical parameters

Hydrophobicity (H) was calculated using HeliQuest²³ (effects of FITC were omitted, β -Ala were replaced by Gly). The isoelectric point (IP) was calculated using GenScript. IsoAsp and 2,3-diaminopropionic acid (Dap) were replaced by Asn and Ala respectively. Linear regression was conducted using SPSS 22.0 (IBM).

Cell viability

The adherent cells were seeded in 96-well plates and allowed to grow in medium supplemented with 10% FBS overnight. The cells were incubated with a serial dilution of peptides at 310 K in 5% FBS containing media for 48 h supplied with 5% CO_2 . Then, 20 μL of the 3-(4,5-dimethyl-2-thiazolyl)-2,5-diphenyltetrazolium bromide (MTT) reagent was added and incubated at 310 K for 4 h. The absorbance of the formazan product was measured at 490 nm by using a microplate reader (Perkin Elmer).

Conclusions

In this report, we studied the factors contributing to the cell penetration and nucleus translocation of N-terminal cross-linked aspartic acid stabilized amphiphilic peptides. The peptides penetrate cells *via* a mixed mechanism. Addition of residues like Trp, Phe and Arg, and increasing the hydrophobicity or isoelectric point of stabilized peptides will improve their cell penetration and nucleus translocation. Finally, the derived peptides with high cell penetration and nucleus translocation are potentially applicable for drug delivery. This study helps to understand and predict the cell penetration and nucleus translocation of stabilized helical peptides.

Acknowledgements

This work is supported by the Natural Science Foundation of China (21372023 and 81572198), the Ministry of Science and Technology of the People's Republic of China (2015DFA31590), and the Shenzhen Science and Technology Innovation Committee (JSGG20140519105550503, JCYJ20150331100849958, JCYJ20150403101146313, JCYJ20160301111338144, JCYJ20160331115853521, JSGG20160301095829250, and KQTD201103).

References

- 1 L. G. Milroy, T. N. Grossmann, S. Hennig, L. Brunsveld and C. Ottmann, *Chem. Rev.*, 2014, **114**, 4695–4748.
- 2 T. A. Hill, N. E. Shepherd, F. Diness and D. P. Fairlie, *Angew. Chem., Int. Ed.*, 2014, **53**, 13020–13041.
- 3 C. E. Schafmeister, J. Po and G. L. Verdine, *J. Am. Chem. Soc.*, 2000, **122**, 5891–5892.
- 4 R. N. Chapman, G. Dimartino and P. S. Arora, *J. Am. Chem. Soc.*, 2004, **126**, 12252–12253.
- 5 N. E. Shepherd, H. N. Hoang, G. Abbenante and D. P. Fairlie, *J. Am. Chem. Soc.*, 2005, **127**, 2974–2983.
- 6 A. M. Spokoyniy, Y. Zou, J. J. Ling, H. Yu, Y.-S. Lin and B. L. Pentelute, *J. Am. Chem. Soc.*, 2013, **135**, 5946–5949.
- 7 Y. H. Lau, P. de Andrade, S.-T. Quah, M. Rossmann, L. Laraia, N. Skold, T. J. Sum, P. J. E. Rowling, T. L. Joseph,

- C. Verma, M. Hyvonen, L. S. Itzhaki, A. R. Venkitaraman, C. J. Brown, D. P. Lane and D. R. Spring, *Chem. Sci.*, 2014, **5**, 1804–1809.
- 8 L. D. Walensky, A. L. Kung, I. Escher, T. J. Malia, S. Barbuto, R. D. Wright, G. Wagner, G. L. Verdine and S. J. Korsmeyer, *Science*, 2004, **305**, 1466–1470.
- 9 A. M. Leduc, J. O. Trent, J. L. Wittliff, K. S. Bramlett, S. L. Briggs, N. Y. Chirgadze, Y. Wang, T. P. Burris and A. F. Spatola, *Proc. Natl. Acad. Sci. U. S. A.*, 2003, **100**, 11273–11278.
- 10 T. Nagakubo, Y. Demizu, Y. Kanda, T. Misawa, T. Shoda, K. Okuhira, Y. Sekino, M. Naito and M. Kurihara, *Bioconjugate Chem.*, 2014, **25**, 1921–1924.
- 11 D. Mandal, A. Nasrolahi Shirazi and K. Parang, *Angew. Chem., Int. Ed.*, 2011, **50**, 9633–9637.
- 12 R. M. Martin, G. Ter-Avetisyan, H. D. Herce, A. K. Ludwig, G. Lattig-Tunnemann and M. C. Cardoso, *Nucleus*, 2015, **6**, 314–325.
- 13 H. Zhao, Q. S. Liu, H. Geng, Y. Tian, M. Cheng, Y. H. Jiang, M. S. Xie, X. G. Niu, F. Jiang, Y. O. Zhang, Y. Z. Lao, Y. D. Wu, N. H. Xu and Z. G. Li, *Angew. Chem., Int. Ed.*, 2016, **55**, 12088–12093.
- 14 G. J. Hilinski, Y. W. Kim, J. Hong, P. S. Kutchukian, C. M. Crenshaw, S. S. Berkovitch, A. Chang, S. Ham and G. L. Verdine, *J. Am. Chem. Soc.*, 2014, **136**, 12314–12322.
- 15 G. Lattig-Tunnemann, M. Prinz, D. Hoffmann, J. Behlke, C. Palm-Apergi, I. Morano, H. D. Herce and M. C. Cardoso, *Nat. Commun.*, 2011, **2**, 453.
- 16 R. Wallbrecher, L. Depre, W. P. Verdurmen, P. H. Bovee-Geurts, R. H. van Duinkerken, M. J. Zekveld, P. Timmerman and R. Brock, *Bioconjugate Chem.*, 2014, **25**, 955–964.
- 17 G. H. Bird, E. Mazzola, K. Opoku-Nsiah, M. A. Lammert, M. Godes, D. S. Neuberg and L. D. Walensky, *Nat. Chem. Biol.*, 2016, **12**, 845–852.
- 18 M. L. Jobin, M. Blanchet, S. Henry, S. Chaignepain, C. Manigand, S. Castano, S. Lecomte, F. Burlina, S. Sagan and I. D. Alves, *Biochim. Biophys. Acta*, 2015, **1848**, 593–602.
- 19 Z. Qian, A. Martyna, R. L. Hard, J. Wang, G. Appiah-Kubi, C. Coss, M. A. Phelps, J. S. Rossman and D. Pei, *Biochemistry*, 2016, **55**, 2601–2612.
- 20 C. Sinthuvanich, A. S. Veiga, K. Gupta, D. Gaspar, R. Blumenthal and J. P. Schneider, *J. Am. Chem. Soc.*, 2012, **134**, 6210–6217.
- 21 H. Yamashita, Y. Demizu, T. Shoda, Y. Sato, M. Oba, M. Tanaka and M. Kurihara, *Bioorg. Med. Chem.*, 2014, **22**, 2403–2408.
- 22 Q. Chu, R. E. Moellering, G. J. Hilinski, Y.-W. Kim, T. N. Grossmann, J. T. H. Yeh and G. L. Verdine, *MedChemComm*, 2015, **6**, 111–119.
- 23 R. Gautier, D. Douguet, B. Antonny and G. Drin, *Bioinformatics*, 2008, **24**, 2101–2102.